



Publication Year	2018
Acceptance in OA	2020-11-03T16:55:23Z
Title	Unusual polarimetric properties of (101955) Bennu: similarities with F-class asteroids and cometary bodies
Authors	CELLINO, Alberto, Bagnulo, S., Belskaya, I. N., Christou, A. A.
Publisher's version (DOI)	10.1093/mnrasl/sly156
Handle	http://hdl.handle.net/20.500.12386/28138
Journal	MONTHLY NOTICES OF THE ROYAL ASTRONOMICAL SOCIETY. LETTERS
Volume	481

Unusual polarimetric properties of (101955) Benu: similarities with F-class asteroids and cometary bodies

A. Cellino,^{1★} S. Bagnulo,^{2★} I. N. Belskaya^{3★} and A. A. Christou²

¹INAF - Osservatorio Astrofisico di Torino, I-10025 Pino Torinese, Italy

²Armagh Observatory and Planetarium, College Hill, Armagh BT61 9DG, UK

³Institute of Astronomy of V.N. Karazin Kharkiv National University, Sum'ska Str. 35, Kharkiv UA-61022, Ukraine

Accepted 2018 August 23. Received 2018 August 10; in original form 2018 July 15

ABSTRACT

We have obtained polarimetric measurements of asteroid (101955) Benu, a presumably primitive near-Earth object (NEO) that is the target of NASA's sample return mission OSIRIS-REx. During our observing campaign, Benu was visible from Earth under a wide range of illumination conditions, with phase angle in the range 16° – 57° . Together with (3200) Phaethon and (152679) 1998 KU2, observed very recently, Benu is the only existing example of a primitive NEO observed in polarimetric mode over a wide interval of phase angles. Based on our polarimetric data, we propose that Benu belongs to the unusual *F* taxonomic class defined in the 80s. According to previous works, the *F*-class includes objects with cometary features. This fact can be of great importance for the interpretation of the results of the exploration of this object by OSIRIS-REx. From polarimetry we also derive an estimate of the geometric albedo of Benu: $p_R = 0.059 \pm 0.003$.

Key words: polarization – minor planets, asteroids: general.

1 INTRODUCTION

Asteroid (101955) Benu is the asteroid target of the OSIRIS-REx space mission (Lauretta et al. 2017). From ground-based observations, we know that this object is 550 metres in size and has a rather spheroidal shape (Lauretta et al. 2015, and references therein). By applying to radar and thermal IR observations a sophisticated thermophysical model, Yu & Ji (2015) found for Benu a geometric albedo of $0.047^{+0.008}_{-0.001}$, and a thermal inertia suggesting a surface covered by a fine-grained regolith. Its spectral reflectance properties make Benu a member of the *B* taxonomic class, according to the SMASS-based classification by Bus & Binzel (2002). Benu was chosen as the target of OSIRIS-REx because it satisfied some basic requirements: it is representative of the population of primitive, low-albedo asteroids orbiting in the inner Solar System, which are thought to be the parent bodies of the most ancient classes of primitive meteorites, including Carbonaceous Chondrites. Moreover, it has a very suitable orbit for a sample-return mission.

The modern *B* taxonomic class as defined by Bus & Binzel (2002) (SMASS taxonomy) includes asteroids that in the 80s were classified into two separate classes, named *B* and *F*. These classes were distinguished on the basis of subtle differences in the spectral reflectance behaviour at $\lambda \leq 0.4 \mu\text{m}$. In particular, the *F* class, first proposed by Gradie & Tedesco (1982), exhibits a flat spectropho-

metric trend over the whole interval of covered wavelengths, including the blue region, whereas other classes of objects exhibiting an overall flat spectral trend show a clear decrease of flux shortward of $0.4 \mu\text{m}$ (see fig. 9 of Tholen 1984). Because the bluest spectral region is rarely observed in modern CCD-based spectroscopic surveys, asteroids originally classified as *F* belong now to the modern *B* class defined by Bus & Binzel (2002), characterized by a generally flat or slightly blueish reflectance spectrum over an interval of wavelengths between 0.5 and $1 \mu\text{m}$. For example, asteroid (2) Pallas is the largest member of the *B* class in both the SMASS and in the Tholen's taxonomy, whereas the largest *F*-class asteroid, (704) Interamnia, is *B*-type in the current SMASS taxonomy.

Apart from their spectrophotometric properties, asteroids can be distinguished also by measuring the varying state of polarization of the sunlight scattered by their surfaces in different illumination conditions (see, e.g. Cellino, Gil-Hutton & Belskaya 2015a). The main source of information are the so-called phase-polarization curves, i.e., the polarization value as a function of the phase angle (which is the angle between the Sun, the target, and the observer). Asteroids with similar spectroscopic characteristics often share similar polarimetric properties (Penttilä et al. 2005; Belskaya et al. 2017). There are, moreover, cases in which the polarimetric behaviour sharply characterizes some objects that would be ambiguously characterized based on reflectance spectra. The two most important cases are those of the so-called Barbarians (Cellino et al. 2006), which are beyond the scope of this paper, and of the asteroids previously classified as members of the old *F* taxonomic class (Belskaya et al.

* E-mail: stefano.bagnulo@armagh.ac.uk (S.B.); alberto.cellino@inaf.it (A.C.); irina@astron.kharkov.ua (I.N.B.)

2005). In both cases, we find unusual values of the so-called inversion angle of polarization.

It is known that at small-phase angles, atmosphere-less objects of our Solar system exhibit the phenomenon of so-called ‘negative’ polarization, which means that the scattered sunlight is linearly polarized in the direction parallel to the scattering plane. For the vast majority of asteroids the polarization changes its sign (i.e. becomes perpendicular to the scattering plane) at phase angles $\gtrsim 20^\circ$ (the ‘inversion angle’ α_{inv}). However, in the case of the F-class asteroids, the inversion angle occurs at the distinctly lower phase angle of $\sim 16^\circ$ (Belskaya et al. 2017). Furthermore, the slope of the polarimetric curve around the inversion angle tends to be substantially steeper for F-class asteroids with respect to other taxonomic classes. It is not yet fully understood what physical properties are responsible for such behaviour, but it is believed that it is due to an interplay of composition, refractive index, and sizes of surface regolith particles (Belskaya et al. 2005).

Although no longer retained in modern classification systems, the old distinction between F-class and B-class asteroids is therefore meaningful, and is very interesting also in other respects. Cellino et al. (2001) noted that the Polana family, located in a region of the asteroid main belt which may be an important source of NEOs, includes several F-class members (Bottke et al. 2015; De León et al. 2018). Perhaps more interestingly, the peculiar polarimetric properties of the F-class asteroids, in particular a low value of the polarimetric inversion angle, seem to be shared also by cometary nuclei, in a few cases of polarimetric measurements of cometary nuclei observed in conditions of absence of the coma (Stinson 2017). In the past, the object (4015) Wilson-Harrington, originally discovered and classified as an F-class asteroid in 1992, was later found to exhibit cometary activity (see Fernandez et al. 1997, and references therein). 133P/Elst-Pizarro, an object described as either an active asteroid or a cometary object in the main asteroid belt, which exhibits recurrent cometary activity, was also found by Bagnulo et al. (2010) to exhibit a low value of the inversion angle of polarization. There is therefore some evidence that at least a subset of the old F-class asteroids may include active, or sporadic, or nearly extinct (as in the case of Wilson-Harrington) comets (see also Belskaya et al. 2015; Cellino et al. 2015a).

Knowing that it was classified as B-class, we have decided to carry out a polarimetric investigation of (101955) Benu, and perform a comparison with the polarimetric properties of F-type objects.

2 OBSERVATIONS

Broad-band linear polarization measurements of (101955) Benu were obtained using the FORS2 instrument (Appenzeller et al. 1998) of the ESO Very Large Telescope (VLT) in the *R* special filter (centred at 655 nm, $FWHM = 165$ nm), which was chosen to maximize the S/N ratio. During ESO period P100 (in 2018 February and March) we obtained three FORS2 polarimetric measurements at large phase-angles. This data set was then complemented with three additional measurements obtained in 2018 May and June thanks to Director Discretionary Time. Observations were acquired using the beam-swapping technique (see e.g. Bagnulo et al. 2009), which consists of obtaining flux measurements at different position angles of the $\lambda/2$ retarder waveplate: 0° , 22.5° , ..., 157.5° . Data reduction was performed as described in detail in section 2.2 of Bagnulo et al. (2016). Throughout this paper, we will refer to the reduced Stokes parameter $P_Q = Q/I$ representing the flux perpendicular to the plane Sun–Object–Earth (the scattering plane) minus the flux parallel to that plane, divided by the sum of the two fluxes. For symmetry

reasons, the reduced Stokes parameter $P_U = U/I$ is expected to be zero. In fact, in two observing epochs (2018 February 19 and 20) the instrument position angle was set parallel to the scattering plane, and only P_Q was measured, under the assumption that the polarization was either perpendicular or parallel to the scattering plane (this condition is nearly always satisfied for all asteroids at all phase angles). As an additional quality check, we provided null parameters N_Q and N_U , which are expected to be consistent with zero within error bars (Bagnulo et al. 2009).

The observing log and our measurements are given in Table 1, and plotted in Fig. 1, together with literature measurements of other objects as discussed in Section 3.

3 ANALYSIS

A comparison of our polarimetric data of Benu with literature data of other asteroids is not straightforward because most polarimetric measurements have been obtained for main-belt asteroids that cannot be observed at phase angles $\gtrsim 30^\circ$. At these phase angles, differences in the polarimetric behaviour of objects of different classes may be firmly detected only when several data points measured with accuracy better than ~ 0.1 per cent are available. Asteroid Benu is faint ($V \gtrsim 20$), and even with a 8 m class telescope it was not possible to densely monitor its polarimetric behaviour with phase angle with uncertainties smaller than 0.1–0.15 per cent. In the positive branch, linear polarization increases significantly with phase angle, and at $\alpha \gtrsim 30^\circ$, corresponding to most of our observations of Benu, the differences between the polarimetric curves of asteroids of different spectral classes may be detected with lower S/N measurements, but literature data are scarce to make a statistically meaningful comparison with other known objects.

We should also remind the reader that most polarimetric observations of asteroids were obtained in the *V* filter, while Benu was observed in the *R* special filter. Therefore some caution is needed to make a comparison between our data and those from previous literature. Spectropolarimetry of asteroid (2) Pallas by Bagnulo, Cellino & Sterzik (2015) shows that in the positive branch, both at $\alpha = 22.9^\circ$ and $\alpha = 27.5^\circ$, polarization is nearly constant with wavelength in the optical up to 900 nm. A similar property was also found by Devogèle et al. (2018) for the B-type asteroid (3200) Phaethon at phase angles similar to those of our observations of Benu. Furthermore, Gil-Hutton, Cellino & Bendjoya (2014) presented thirty-eight polarimetric observations of seven asteroids belonging to the SMASS-based B-class, and they merged together *V* and *R* data in building averaged phase-polarization curves for these objects, since no systematic difference was found for data taken in the two different colours. We conclude that our polarimetric observations in the *R* band may be compared meaningfully with those of literature data of F-type and B-type asteroids obtained both in *R* and in *V* filters.

In our analysis, we have fit our polarimetric data of Benu with the linear-exponential function

$$P_Q(\alpha) = A \left(e^{-(\alpha/B)} - 1 \right) + C \alpha \quad (1)$$

This is a three-parameter relation issued from a semi-empirical modelling that Kaasalainen et al. (2003) found to be suited to fit both phase-magnitude relations in asteroid photometry, and phase-polarization curves in asteroid polarimetry (see also Cellino et al. 2015b; Belskaya et al. 2017, and references therein). In equation (1), α is the phase angle, and A , B , and C are free parameters. The red solid-line in Fig. 1 shows our best fit obtained with equation (1) together with $\pm 3\sigma$ uncertainties represented by red-dashed lines.

Table 1. Polarimetry of asteroid (101955) Benu in the FORS2 *R* special filter. P_Q and P_U are the reduced Stokes parameters measured in a reference system such that P_Q is the flux perpendicular to the plane Sun–Object–Earth (the scattering plane) minus the flux parallel to that plane, divided by the sum of the two fluxes.

Date (yyyy mm dd)	Time (UT) (hh:mm)	Exp (sec)	Phase angle (DEG)	P_Q (%)	P_U (%)	N_Q (%)	N_U (%)
2018 02 19	08:37	2760	57.12	21.05 ± 0.56	–	-0.48 ± 0.56	–
2018 02 20	08:09	5520	56.90	20.78 ± 0.48	–	-0.46 ± 0.48	–
2018 03 18	06:39	4400	49.56	15.51 ± 0.33	-0.36 ± 0.30	0.46 ± 0.33	-0.11 ± 0.30
2018 03 21	06:52	4400	48.43	15.34 ± 0.45	-0.28 ± 0.50	-0.22 ± 0.45	0.73 ± 0.50
2018 05 12	03:31	3520	15.96	-0.52 ± 0.12	-0.17 ± 0.12	0.30 ± 0.12	0.14 ± 0.12
2018 06 11	01:58	3520	27.89	3.95 ± 0.16	0.14 ± 0.13	-0.02 ± 0.16	-0.15 ± 0.13
2018 06 16	00:37	3520	31.24	5.19 ± 0.14	-0.44 ± 0.14	-0.14 ± 0.14	-0.16 ± 0.14

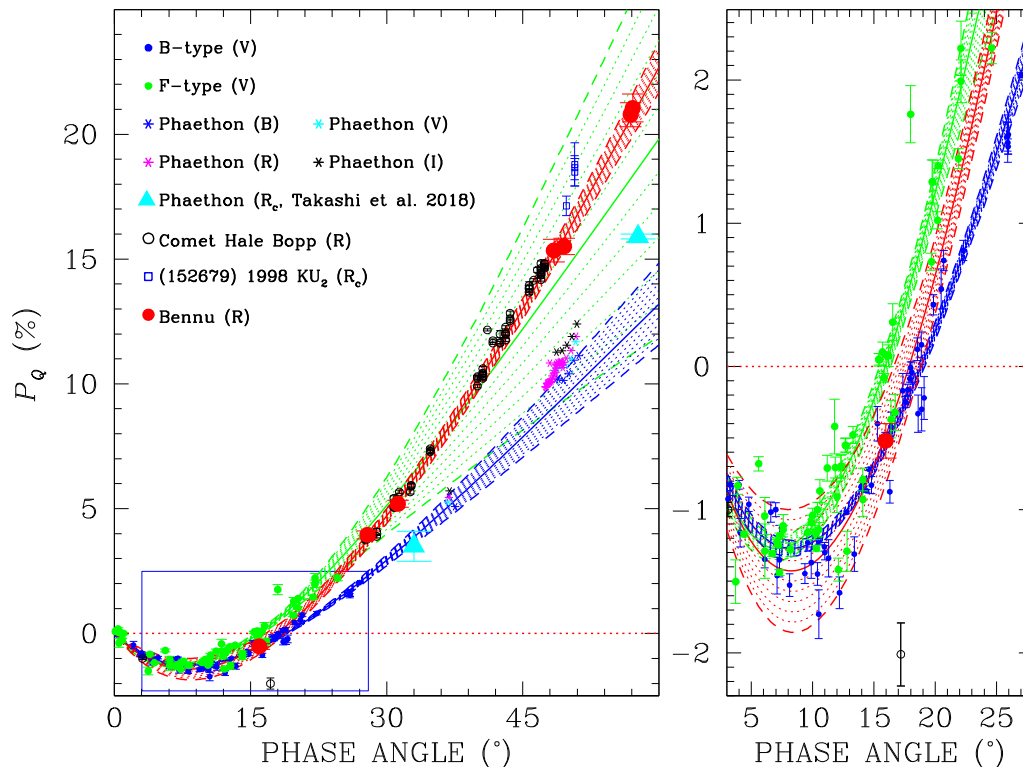


Figure 1. Polarization versus phase angle for asteroid Benu compared with B-class and F-class main belt asteroids, near-Earth asteroids (3200) Phaethon and (152679) 1998 KU₂, and comet Hale–Bopp. Key to the symbols is given in the left-hand panel. Solid lines and dotted areas delimited by dashed lines show the best fits and 3σ boundaries to data for Benu (red lines), B (blue lines), and F (green lines) asteroids.

Using equation (1) we have built two synthetic phase-polarization curves by merging literature data of asteroids (2), (24), (47), (59), (431), and (702) for the B-class, and asteroids (213), (225), (302), (419), (704), and (762) for the F-class (taxonomy classification from NASA *Planetary Data System* maintained by C. Neese and available at <http://pds.jpl.nasa.gov/>, and data from Gil-Hutton & Cañada-Assandri 2011, 2012; Cañada-Assandri, Gil-Hutton & Benavidez 2012; Gil-Hutton, Cellino & Bendjoya 2014; Belskaya et al. 2017). Our sample of B-class asteroids was collected using objects that were classified as B both in SMASS and in the Tholen system; the sample of F-class asteroids was built using only ‘pure’ F-objects in the Tholen’s classification, that is, without considering objects classified as FC, CF, or similar ambiguous cases. Data points for B-class and F-class asteroids, together with their best fits, are shown in Fig. 1. Best-fitting parameters for all these curves are given in Table 2.

The inversion angle (constrained by just one single point in the negative polarization branch) is between the value of $\sim 16^\circ$ and $\sim 19^\circ$, which are typical for the F-class and B-class, respectively. We note, however, that the α_{inv} values of two F-class asteroids determined by Belskaya et al. (2017) are actually $\gtrsim 17^\circ$, fully consistent with the value for Benu. Based on its α_{inv} value, Benu could be either a B-class or an F-class asteroid.

Due to the shortage of data points in the negative branch, the slope at the inversion angle, $dP_Q/d\lambda(\alpha = \alpha_{\text{inv}})$, and (even more) the $P_Q^{(\text{min})}$ parameters are not well constrained. The slope, however, is closer to the values displayed by F-class asteroids.

Taking at face value our best-fitting solution, we can also in principle derive an estimate of the geometric albedo of Benu. Since $P_Q^{(\text{min})}$ is poorly determined and the trend in the positive polarization branch seems to be not very linear, and might lead us to use an exceedingly steep estimate, we prefer to use here the relation

Table 2. Best-fitting parameters.

OBJECT	α_{inv} ($^{\circ}$)	α_{min} ($^{\circ}$)	$P_Q^{(\text{min})}$ (%)	Slope (%/ $^{\circ}$)
Bennu	17.88 ± 0.40	8.28 ± 0.13	-1.43 ± 0.14	0.276 ± 0.012
B class	18.86 ± 0.09	8.26 ± 0.10	-1.27 ± 0.02	0.210 ± 0.003
F class	15.93 ± 0.15	7.15 ± 0.22	-1.27 ± 0.03	0.260 ± 0.008

proposed by Cellino et al. (2015b) between the albedo and the so-called Ψ parameter, defined as $\Psi = P_Q(30^{\circ}) - P_Q(10^{\circ})$. We found for Bennu $\Psi = 6.083 \pm 0.266$ and a corresponding formal solution for the albedo of 0.059 ± 0.003 . This value, to be confirmed when a better sampling of the phase-polarization curve is available, fits nicely the value found for the F-class by Belskaya et al. (2017), namely 0.058 ± 0.011 . The same authors found for the B-class an average albedo of 0.083 ± 0.034 . By using the Ψ parameter and the data shown in Fig. 1, we found for the B and F classes the values of 0.085 ± 0.004 and 0.057 ± 0.014 , respectively.

Four of our seven data points for Bennu were taken at phase angle $>40^{\circ}$. Our best fits for B and F asteroids may be extrapolated at larger phase angles, and Fig. 1 clearly shows that Bennu's data are much more consistent with what predicted for F-class rather than B-class asteroids.

4 DISCUSSION AND CONCLUSIONS

Until recently, a meaningful comparison with data for other asteroids at large-phase angles would not have been possible, because only a few moderate- or high-albedo near-Earth asteroids, supposed to have a completely different thermal history and composition than Bennu, had been observed. However, very recently Ito et al. (2018) and Devogèle et al. (2018) carried out polarimetric observations of the NEO (3200) Phaethon at very large phase angles. The analysis of their data led Devogèle et al. (2018) to conclude that Phaethon is most likely a collisional fragment of the B-class asteroid (2) Pallas, in particular a fugitive from Pallas' family, confirming previous results based exclusively on spectral reflectance data by De León et al. (2010). The observations by Devogèle et al. (2018) and Ito et al. (2018) are also shown in Fig. 1. We note that at phase angles $\sim 100^{\circ}$ (not shown in Fig. 1), the two polarimetric datasets are not consistent: around phase angle 105° , polarization values from Ito et al. (2018) reach about 50 per cent while at phase angle 101° , Devogèle et al. (2018) measure only 38 per cent. An explanation for this discrepancy, possibly due to surface heterogeneity of Phaethon, is beyond the scope of this paper. However, at phase angles $\lesssim 60^{\circ}$, it clearly appears that Bennu exhibits values of linear polarization much higher than those of Phaethon. Our measurements, as well as the very recent observations of (152679) 1998 KU2 (Kuroda et al. 2018) are the highest ever found for a NEO observed at large phase angles. Another Solar system object that exhibits such high-polarization values is comet C/1995 O1 (Hale-Bopp), which was observed by Manset & Bastien (2000) in a 9 nm wide gas-free filter centred around $\lambda = 694$ nm. Hale-Bopp measurements are also shown in Fig. 1. The resemblance between the polarimetric data of Bennu and those of Hale-Bopp is striking, and although reinforces the conclusion about similarity between F-type objects and cometary dust proposed by Kolokolova & Jockers (1997), it should be treated with caution, due to the big differences between the two physical environments: in one case we have an obviously active and very large comet, in the other one a much smaller asteroid with no detection of a gas or dust coma.

Our data show that the phase-polarization curve of Bennu is steeper than the extrapolation of phase-polarization curves of main-belt B-class asteroids observed at phase angles $\lesssim 30^{\circ}$, and resembles that of F-class asteroids. At phase angles $\lesssim 30^{\circ}$, the polarimetric behaviour of Bennu is probably in between that typical of the F and B classes. Dynamical modelling has suggested that Bennu has most likely have evolved from the Inner part of the Main Belt (IMB; $a < 2.5$ au; Walsh et al. 2013, and references therein) possibly within either the 'New' Polana or Eulalia families (Bottke et al. 2015). If this is true, taking into account the finding by Cellino et al. (2001) that most of Polana family's members belong to the F-class, our polarimetry might support the hypothesis that Bennu originated in that family, since Eulalia is a C-class asteroid.

Based on what is currently known about the similarity in polarimetric behaviour of the asteroid F-class and of some cometary bodies, (101955) Bennu could be compatible with cometary characteristics and a possible cometary origin. According to DeMeo & Binzel (2008), the estimated fraction of comets likely present in the NEO population should be 8 ± 5 per cent. In a search for such objects, NEOs exhibiting the typical behaviour of the F-class should be considered as highest priority candidates, because, whatever can be the physical or evolutionary mechanism causing an anomalously low value of the polarization inversion angle, this rare property is shared by at least a few bodies belonging to the cometary population and by others belonging to the asteroid F taxonomic class.

We note that the conventional separation between asteroids and comets has become increasingly uncertain in recent years, also after the discovery of the so-called main belt comets (Hsieh & Jewitt 2006). It is possible that the target of OSIRIS-REx is an object borderline between typical asteroids and typical comets (Novaković et al. 2012; Novaković, Hsieh & Cellino 2014). A possible link with cometary objects would have obvious consequences about the interpretation of the future *in situ* exploration of Bennu by OSIRIS-REx and of the sample of material brought back to the Earth. Moreover, we note that Bennu is also one of the few objects for which an accurate measurement of a Yarkovsky-driven drift in orbital semimajor axis has been obtained (Farnocchia et al. 2013), and used also to calibrate the most recently developed methods of computation of the ages of asteroid dynamical families (Milani et al. 2014, 2017). In this respect, it is clear that the possibility that some (even weak) cometary activity could affect the measurements of a Yarkovsky-driven evolution must be carefully assessed.

ACKNOWLEDGEMENTS

This work is based on observations collected at the European Organization for Astronomical Research in the Southern Hemisphere under ESO programmes 0100.C-0771 and 2101.C-5011.

REFERENCES

Appenzeller I. et al., 1998, *The Messenger*, 94, 1

- Bagnulo S., Landolfi M., Landstreet J. D., Landi Degl'Innocenti E., Fossati L., Sterzik M. F., 2009, *PASP*, 121, 993
- Bagnulo S., Tozzi G. P., Boehnhardt H., Vincent J.-B., Muinonen K., 2010, *A&A*, 514, A99
- Bagnulo S., Cellino A., Sterzik M. F., 2015, *MNRAS*, 446, L11
- Bagnulo S., Belskay I. N., Stinson A., Christou A., Borisov G. B., 2016, *A&A*, 585, A122
- Belskaya I. N. et al., 2005, *Icarus*, 178, 213
- Belskaya I. N., Cellino A., Gil-Hutton R., Muinonen K., Shkuratov Yu. G., 2015, in Michel P., DeMeo F., Bottke W. F., eds, *Asteroids IV*, Univ. of Arizona Press, Tucson, p. 151
- Belskaya I. N. et al., 2017, *Icarus*, 284, 30
- Bottke W. F. et al., 2015, *Icarus*, 247, 191
- Bus S. J., Binzel R., 2002, *Icarus*, 158, 146
- Cañada-Assandri M., Gil-Hutton R., Benavidez P., 2012, *A&A*, 542, A11
- Cellino A., Zappalà V., Doressoundiram A., Di Martino M., Bendjoya Ph., Dotto E., Migliorini F., 2001, *Icarus*, 152, 225
- Cellino A., Belskaya I. N., Bendjoya P., Di Martino M., Gil-Hutton R., Muinonen K., Tedesco E. F., 2006, *Icarus*, 180, 565
- Cellino A., Gil-Hutton R., Belskaya I. N., 2015a, in Kolokolova L., Hough J., Levasseur-Regourd A.-C., eds, *Polarimetry of stars and Planetary Systems*, Cambridge University Press, Cambridge, UK, p. 300
- Cellino A., Bagnulo S., Gil-Hutton R., Tanga P., Cañada-Assandri M., Tedesco E. F., 2015b, *MNRAS*, 451, 3473
- De León J., Campins H., Tsiganis K., Morbidelli A., Licandro J., 2010, *A&A*, 513, A26
- De León J. et al., 2018, *Icarus*, 313, 25
- DeMeo F. E., Binzel R. P., 2008, *Icarus*, 194, 436
- Devogèle M. et al., 2018, *MNRAS*, 479, 3498
- Farnocchia D., Chesley S. R., Vokrouhlický D., Milani A., Spoto F., Bottke W. F., 2013, *Icarus*, 224, 1
- Fernandez Y. R., McFadden L. A., Lisse C. M., Helin E. F., Chamberlin A. B., 1997, *Icarus*, 128, 114
- Gil-Hutton R., Cañada-Assandri M., 2011, *A&A*, 529, A86
- Gil-Hutton R., Cañada-Assandri M., 2012, *A&A*, 539, A115
- Gil-Hutton R., Cellino A., Bendjoya Ph., 2014, *A&A*, 569, A122
- Gradie J. C., Tedesco E. F., 1982, *Science*, 216, 1405
- Hsieh H. H., Jewitt D., 2006, *Science*, 312, 561
- Ito T. et al., 2018, *Nature Commun.*, 9, 2486
- Kaasalainen S., Piironen J., Kaasalainen M., Harris A. W., Muinonen K., Cellino A., 2003, *Icarus*, 161, 34
- Kolokolova L., Jockers K., 1997, *Planet. Space Sci.*, 45, 1543
- Kuroda D. et al., 2018 *A&A*, 611, A31
- Lauretta D. S. et al., 2015, *Meteorit. Planet. Sci.*, 50, 834
- Lauretta D. S. et al., 2017, *Space Sci. Rev.*, 212, 925
- Manset N., Bastien P., 2000, *Icarus*, 145, 203
- Milani A., Cellino A., Knežević Z., Novaković B., Spoto F., Paolicchi P., 2014, *Icarus*, 239, 46
- Milani A., Knežević Z., Spoto F., Cellino A., Novaković B., Tservoulis G., 2017, *Icarus*, 288, 240
- Novaković B., Hsieh H.H., Cellino A., 2012, *MNRAS*, 424, 1432
- Novaković B., Hsieh H.H., Cellino A., Micheli M., Pedani M., 2014, *Icarus*, 231, 300
- Penttilä A., Lumme K., Hadamcik E., Levasseur-Regourd A.-C., 2005, *A&A*, 432, 1081
- Stinson A. A., 2017, PhD thesis, Queen's University Belfast
- Tholen D. J., 1984, PhD thesis, Univ. Arizona
- Walsh K. J., Delbó M., Bottke W. F., Vokrouhlický D., Lauretta D. S., 2013, *Icarus*, 225, 283
- Yu L., Ji J., 2015, *MNRAS*, 452, 368

This paper has been typeset from a $\text{\TeX}/\text{\LaTeX}$ file prepared by the author.